

SYNTHESIS OF A NEW ADSORBENT BASED ON THE MILD DEALUMINATED BINDER FREE GRANULAR Y ZEOLITE

Dilzhar S. Mohammed a, Farhad M. Ali a, Kanaan R. Ahmed a

a Department of Chemistry, Faculty of Science, University of Zakho, Zakho, Kurdistan Region, Iraq
Dilzhar.Mohammed@stu.uoz.edu.krd; Farhad.ali@uoz.edu.krd; kanaan.ahmed@uoz.edu.krd

Received: 1 Feb., 2023 / Accepted: 14 Apr., 2023 / Published: 12 July 2023

<https://doi.org/10.25271/sjuoz.2023.11.3.1115>**ABSTRACT:**

This study investigates, for the first time, the effects of dealumination of binder-free NaY type zeolite on the adsorption properties and porous structure characteristics. In this study, BF-Y zeolite was hydrothermally synthesized from kaolin and powder NaY. BF-Y was then treated with acid to increase Si/Al ratio. X-ray Diffraction (XRD), Thermal Gravimetric Analysis (TGA), Scanning Electron Microscope (SEM), and Energy Dispersive X-Ray (EDX) have been performed for the characterization. The modified zeolite granules MBF-Y were used as an adsorbent for the removal of methylene blue MB dye from water. The influence of initial MB concentration, contact time, temperature, and adsorbent dosage on adsorption capacity and dye removal percentage on MBF-Y was investigated. The maximum dye removal was attained at a concentration of (8×10^{-6} M) which was more than 93%, and an equilibrium contact time of 60 minutes. Well-known adsorption isotherms (Langmuir, Freundlich, and Tempkin) were used to study the adsorption mechanism of MB onto MBF-Y.

KEYWORDS: NaY Zeolite, Adsorption Capacity, Binder Free Zeolite, Mild Dealumination, Adsorption Isotherms,**1. INTRODUCTION**

Numerous industries, including those that employ dyestuffs, textiles, tanneries, plastics, rubber, paper, and others, unavoidably use more than 10,000 commercially available dyes. More than 10% of yearly manufactured dyes are wasted during their production and processing processes, and about 20% of these lost dyes enter industrial wastewater and cause environmental contamination issues (N. Peng et al. 2016). The effluents of colored dyes may have harmful effects on microorganism populations and may be hazardous or carcinogenic to mammals (Tsai, Hsien, & Hsu, 2009). Different methods such as, coagulation and flocculation (Ihaddaden et al., 2022), physical adsorption, (L. Liu et al., 2015), bio removal (Omar, El-Gendy, & Al-Ahmary, 2018), membrane filtration (Rashidi et al., 2015), and chemical redox reaction (Wu and Wang 2012), had been used for removing dyes from colored waste water. Physical adsorption is among the cheapest and most effective methods used to significantly reduce the amount of dissolved dyes in an effluent. Activated carbon is one of the most commonly used adsorbents for dye removal. However, the synthesis and regeneration processes of activated carbon are very expensive (Wang & Li, 2007). Therefore, the development of other alternative, efficient sorbents with lower costs is still a major challenge (Jiang et al., 2018). High silica zeolite is an efficient adsorbent for the removal of many pollutants, including those in water. Zeolites are micropores of hydrated crystalline aluminosilicates of group (I) and group (II) metals (M. X. Peng et al., 2015). Due to their unique properties, for instance, high thermal and chemical stability, shape selectivity, and adsorption performance, zeolites are used in many applications, such as catalysis processes, adsorption, and ion exchange (Grigorieva et al., 2019).

The catalytic and adsorption performances of zeolites are considerably affected by zeolite crystal size. The crystal size and morphology of zeolite are related to the molar ratio of silicon (Si) to aluminum (Al) (Si/Al). The greater the Si/Al molar ratio, the

greater the particle size and hydrophobicity of zeolite (Shirazi, Jamshidi, & Ghasemi, 2008). Zeolite Y, a very adaptable member of the faujasite (FAU) family, and binder-free granular NaY zeolites are widely used as catalyst in petroleum sections, due to their high surface area and large pore openings. The thermal and hydrothermal stability of this type of zeolite is limited, and acidic Y zeolite partially collapses when exposed to moisture, even at room temperature. The thermal and hydrothermal stability of FAU-Y zeolite is dramatically increased by increasing the Si/Al ratio (McDaniel & Maher, 1968). Dealumination is among the most significant methods used for modifying the Si/Al ratio. It can be done by acid leaching, thermal or hydrothermal treating, and treatment with (Silicon hexafluoride, SiF₆, or Silicon tetrachloride, SiCl₄) (Najar, Zina, & Ghorbel, 2010). Earlier, it was found that, if FAU zeolite is treated with strong inorganic acids such as HCl, the structure of this type of zeolite completely collapses, nevertheless, dilute acid solutions have no significant effect on the crystalline structure of FAU type Y zeolite (Beyer, 2002).

Partial extraction of Al from the Y-type zeolite framework can be done by a controlled mild dealumination process. The extraction of Al leads to the formation of extra framework aluminum species (EFAL) that persist in solids and fill the pores, and the EFAL enhances the catalytic activity and hydrothermal stability of zeolite because it decreases the number of acid sites in zeolite ((Simancas et al. 2021). Some research teams have already investigated the production of different zeolites from kaolin or other fly ashes and have made significant strides toward the synthesis of 4A, mordenite, X, Y, and other zeolites (X. Liu et al., 2003). All previous research papers study the process of

* Corresponding author

This is an open access under a CC BY-NC-SA 4.0 license (<https://creativecommons.org/licenses/by-nc-sa/4.0/>)

dealumination from powdered or granular zeolite, and there are no studies on the removal of aluminium from the binder-free zeolite. Therefore, the main goals of this study are the synthesis of NaY zeolite from kaolin, the synthesis of granular NaY, the modification of the synthesized zeolite by mild dealumination, and the employing of the modified zeolite for the adsorption of the cationic dye methylene blue (MB) from water.

XFNANO Mat. Tech Co., Ltd. with Si/Al of (5.8), 600 m². g⁻¹. Sodium silicate from BDH chemicals Ltd., Poole England. Sodium hydroxide (NaOH) from Labpak Chemicals LTD. Ammonium nitrate (NH₄NO₃) from Labpak Chemicals LTD. Commercial white vinegar from the Zer company in Erbil, Iraq. Table (1) shows the characteristics of raw material:

2. EXPERIMENTAL

2.1. Materials

The Kaolin we used in this work was obtained from Sigma Aldrich with (wt. % 30.9Al; wt. %39.9Si). Powdered NaY from

Sample	Chemical composition (wt%)						Adsorption capacity (mL g ⁻¹)			
	Na	Al	Si	K	Mg	Fe	Si/Al	(benzene)	(n-heptane)	A(Water)
Kaolin	0.0	30.9	37.9	1.1	0.3	0.4	1.80	0.185	0.1420	0.026
Powder NaY	8.2	14.4	43.6	-	-	-	5.84	0.320	0.330	0.195

2.2. Synthesis of Powderd and Granular NaY from Kaolin:

2.2.1. Activation of Kaolin:

Before starting the crystallization process, it is necessary to convert kaolin to its active form, called meta kaolin, by calcination. To do this, 100 g of kaolin were placed in a porcelain crucible and calcined in an oven at 650 °C for four hours. According to Ptáček et al. (2014), conversion of kaolinite to meta-kaolinite is probably achieved at temperatures of 400–650 °C, and decomposition of meta-kaolinite happens at temperatures greater than 950 °C.

2.2.3. Crystallization:

Required amounts of Na₂SiO₃, which is a silicate source, and NaOH solution were added to 10 g of meta-kaolin in a Teflon container and aged at room temperature for 24 hours to increase the degree of crystallinity and Brunauer-Emmett-Teller (BET) surface (Li et al., 2010). After the ageing process, the Teflon container was transferred to a stainless-steel autoclave and crystallized at 100 °C for 5-45 hours. After the crystallization

2.3. Modification

2.3.1. Ion Exchanging of NaY

In a conical flask, the required amount of NH₄NO₃ solution was added to a 10 g zeolite sample, and the flask was placed in a shaker water bath at 80 ± 2 °C with shaking at 150 rpm for one hour. After filtration, the concentration of Na ions in ppm in the filtrate was determined by a Flame Photometer (7PFP7 industrial flame photometer). The remaining solid was then returned to the conical flask, and NH₄NO₃ solution was added. The previous procedure was repeated three times. The concentration of Na ions in both the solid and filtrate was determined in ppm by a flame

2.4. Adsorption Studies

2.4.1. Batch Experiment:

In order to investigate the adsorption characteristics of the synthesised and modified binder-free Y (MBF-Y) zeolite, Methylene Blue (MB) was selected as the model adsorbate. A stock solution of 1 * 10⁻³ M MB was prepared by dissolving 0.32 g of MB in 1 L of deionized water. A stock solution was then used to make solutions at the required concentrations. Batch tests were carried out to examine how different parameters affect the removal process. In a 100 mL quick-fit conical flask, 50 mL of MB solution of known concentration, and an accurately weighed mass of MBF-Y were placed. The conical flask was enclosed by

2.2.2. Preparation of Granules with Binder (GWB):

A paste-like mixture of (30 wt.% kaolin, + 70 wt.% NaY) and about 3 wt. % starch as a pore-forming additive was prepared and granulated by extrusion to form 3-4 mm diameter and 4-6 mm length granules with a binder (GWB). The prepared granules were dried at 120 °C for three hours, then calcined at 650 °C for four hours to convert kaolin to meta-kaolin, in addition of burning starch and removing it as carbon dioxide.

process, solid products were separated from the liquid phase by vacuum filtration, washed with distilled water to a pH of 8.0–9.0 to remove excess NaOH solution, and dried at 120 °C for 3 hours. The same procedure was used to prepare powdered NaY from a mixture of meta-kaolin and 10% seed and granules prepared from 30% kaolin and 70% powdered NaY.

photometer and converted to an ion exchange weight percentage. The adsorption capacity of ion-exchanged samples was determined.

2.3.2. Mild Dealumination:

Five grams of the NH₄Y-form Zeolite sample were placed in a 1L conical flask with 500 mL of commercial vinegar containing 0.75 M ethanoic acid. The conical flask was sealed with a rubber stopper and shaken for 0.5, 1, 1.5, 2, 2.5, and 3 hours in a water bath at 90 °C with 150 RPM. After filtration and washing the solid with one liter of hot water, the dealuminated sample was dried in an oven at 80 °C for 3 hours.

a glass stopper. The mixture was placed in a temperature-controlled shaker at 25 °C and 150 rpm. After appropriate intervals, an aliquot of the mixture was centrifuged for three minutes at 2000 rpm. A UV-Visible spectrophotometer, Perkin Elmer at 665.99 nm, with a deionized water blank, quartz cuvette, was used to determine the remaining dye concentration in the supernatant at 2000 rpm. A UV-Visible spectrophotometer, Perkin Elmer at 665.99 nm, with a deionized water blank, quartz cuvette, was used to determine the remaining dye concentration in the supernatant (Ismail et al., 2022). Equation 1 (A. Manzoli et al., 2020) was applied to calculate the equilibrium

adsorption capacity, and dye removal percentage efficiency was calculated by equation 2 (M. Shirani et al., 2014).

$$q_e = \left(\frac{C_i - C_e}{m} \right) * V \quad (1) \text{ (Rida, Bouraoui, and Hadnine 2013)}$$

$$\text{Dye removal \%} = \left(\frac{C_i - C_e}{C_i} \right) * 100, \dots (2) \text{ (L. Liu et al. 2015)}$$

where C_i is the initial concentration of MB solution in M at time 0. C_e is the equilibrium concentration of MB dye in (M), at equilibrium time (80min). V is the volume of solution in L, m is the mass of the adsorbent in g, and q_e is the equilibrium adsorption capacity in mol g^{-1} . All experiments were repeated three times, and the average of the data obtained was used for calculations. In order to determine the effect of initial dye concentration and adsorption isotherms, solutions of MB with different concentrations in the range of $6.5 * 10^{-6}$ to $2 * 10^{-5}$ M were mixed with accurately weighed 0.01 g of MBF-Y. The effect of MBF-Y dosage was determined by mixing different masses of MBF-Y with 50 mL of $1 * 10^{-5}$ M MB solution for 80 min. Additionally, in order to determine the effect of contact time and adsorption kinetics, 0.01 g of MBF-Y was subjected to a 50 mL solution of MB $1 * 10^{-5}$ M for selected time intervals from 5 to 80

4. RESULTS AND DISCUSSION

4.1. Synthesis of Powdered NaY Zeolite from Meta kaolin

Table 2 illustrates the results of the crystallization of the meta-kaolin without using seeds. According to the results of a preliminary experiment on the synthesis of powdered Y zeolites from meta-kaolin, which is similar to the process of synthesis of zeolites of this structural type from silica-alumina hydrogels (Pavlov et al., 2015). The zeolite cannot be formed unless X-ray crystal seeds are added to the reaction mixture, and this is exactly what happened in this study, where the degree of crystallinity did

min. Adsorption thermodynamics and the effect of temperature on adsorption capacity and the percentage of dye removal efficiency were also determined at four different temperatures 298, 303, 313, and 323 K on a mixture of $1 * 10^{-5}$ M MB solution and 0.01 g MBF-Y.

3. CHARACTERIZATION

X-Ray Powder Diffraction (XRD) with a high-resolution Powder X-ray Diffractometer, 9 kW (40 KV, 450 mA) was used to determine the phase composition and degree of crystallinity. The chemical composition of samples was determined using Energy Dispersive X-Ray (EDX). The nitrogen adsorption/desorption method was used to determine the BET surface area and total pore volume of zeolite samples. Thermogravimetric analysis or TGA, was used to determine thermal weight loss. The static adsorption capacities A of zeolites for water vapour, benzene, and n-heptane, were determined in $mL g^{-1}$ under static conditions by the "desiccator method" at $25^\circ C$ and $p/p_s = 0.7-0.8$ (Sing, Rouquerol, & Rouquerol, 2013).

not exceed 24% and values of adsorption capacity were very low. Table 3 shows the effect of using 10% seed crystals at $100^\circ C$ on the synthesis of powdered NaY from calcined kaolin according to the reaction mixture mentioned before. The crystallization process was carried out at $25^\circ C$ for 24 hours and subsequently at $100^\circ C$ for 5- 45 hours. From the results manifested in Table (3), it is clear that after 40 hours of the crystallization process, zeolite was obtained with a high degree of crystallinity (94.68%) and a good value of adsorption of benzene, n-heptane, and water vapour.

Table 3. crystallization of NaY from meta-kaolin using 10% seed crystals

Crystallisation time(h)	Degree of crystallinity (%)	Adsorption capacity (A) ($mL g^{-1}$)		
		A(benzene)	A(n-heptane)	A(water)
5	43.43	0.139	-	-
10	42.81	0.137	-	-
15	50.31	0.161	-	-
20	48.43	0.155	-	-
30	52.50	0.168	-	-
35	55.93	0.179	0.211	0.117
38	85.93	0.275	0.254	0.192
40	94.68	0.303	0.314	0.192
45	93.75	0.300	0.319	0.183

4.2. Synthesis of Binder Free NaY (BF-Y) Granules

According to the preliminary experiment on the synthesis of granular Y zeolite without binder, about 55 wt% to 75 wt.% powdered Y zeolite should be admixed with kaolin and a pore-forming additive to prepare binder-free granules with high mechanical strength, adsorption capacity, and degree of crystallinity (Pavlov et al. 2015). In our case, we mixed (70 wt.%) of powdered NaY zeolite with (30 wt.%) of kaolin and about (3 wt.%) starch (pore-forming additive). It was vital to ascertain the circumstances under which kaolin converts into this zeolite because kaolin was present in the first granules during the crystallization of granules with the binder (GWB). The results of the adsorption capacity obtained from Table (3) are good pieces of evidence for the conversion of kaolin into powdered NaY after 40 hours of crystallization at $100^\circ C$ under the conditions described above. The crystallization process of GWB for the

synthesis of BF-Y was carried out at $25^\circ C$ for 24 hours and subsequently at $100^\circ C$ for 10-45 hours. Table (4) presents the data on the effect of duration at $100^\circ C$ on the synthesis of GBF-Y. As can be seen from Table 4, 40 hours under these circumstances is plenty to achieve the maximal degree of crystallinity (98%). It is noticeable from the adsorption capacity values of benzene vapour for BF-Y ($0.31 mL g^{-1}$) and powdered zeolite ($0.32 mL g^{-1}$), that the GWB after the 40-hour crystallization process at $100^\circ C$ transformed a large part of it (with a percentage of up to 98%) into BF-Y type materials. Furthermore, more than 96% of the GWB was converted into BFG-Y type materials based on the n-heptane vapour adsorption capacities values in Table 4: $0.32 mL g^{-1}$ for BFG-Y and $0.33 mL g^{-1}$ for powdered

NaY after 40 hours of crystallization at 100 °C. The increase in the time of the crystallization process leads to the formation of the amorphous model, as noted in Table (4) from the value of the adsorption capacities (especially water and n-heptane), and also from the X-ray data. According to XRD data, Figure 1 pattern (b), the diffractogram of BF-Y formed after 40 hours 'crystallization is completely similar to the diffractogram of powdered NaY zeolite pattern (a), and this is a good indication

that a large proportion of clay has been transformed into zeolite. According to XRD data in Figure 1 pattern (d), acid treatment of BF-Y after 1.5 hour partially amorphizes the zeolite crystal lattice due to its dealumination. Increasing the crystallization time to 45 hours leads to an increase in the amorphous ratio due to the dissociation of the crystalline structural elements (see Figure 1 pattern (c)).

Table 4. Effect of the duration of the crystallization on the binder free granules Y zeolite (BF-Y).

Sample	Aging time (h)	Crystallization time(h)	Adsorption capacity (mL g ⁻¹)			Degree of crystallinity(%)	Total pore volume (mL.g ⁻¹)	Si/Al
			A(benzene)	A(n-heptane)	A(water)			
NaY	0	0	0.32	0.33	0.195	100	0.51	5.84
GBW	0	0	0.122	0.131	0.24	38.12	0.18	4.43
GBW	24	10	0.05	0.08	0.02	15.62	0.07	-
		15	0.06	0.06	0.02	18.75	0.08	-
		20	0.08	0.07	0.02	25.00	0.10	-
		25	0.08	0.09	0.02	25.00	0.10	-
		30	0.09	0.10	0.03	28.12	0.12	-
		35	0.23	0.28	0.06	71.87	0.29	-
		40	0.31	0.32	0.09	98.00	0.40	4.01
		45	0.24	0.23	0.02	74.00	0.03	-

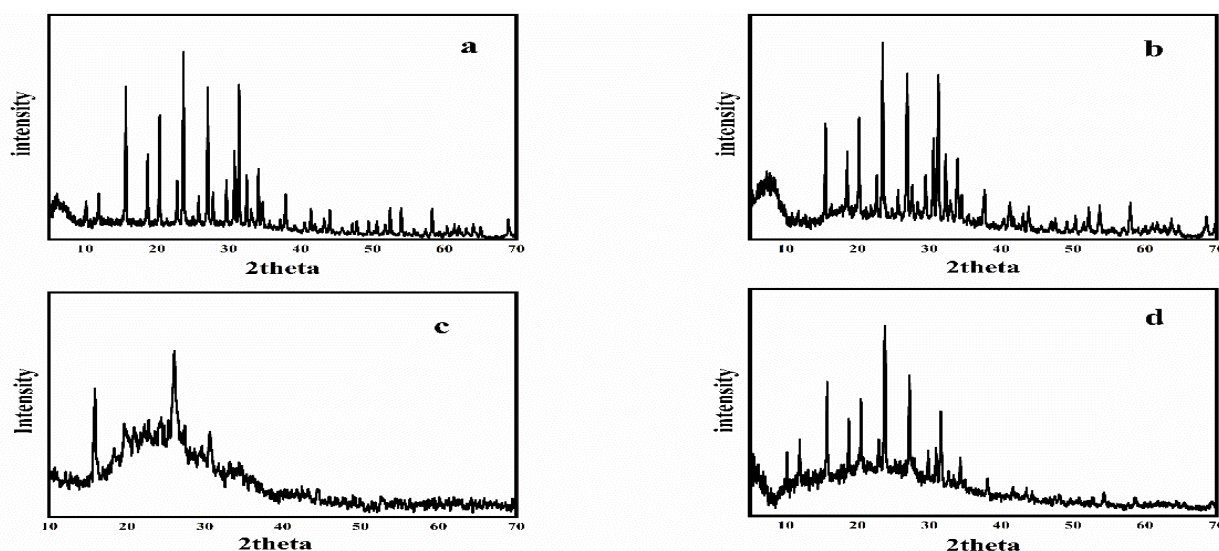
4.3. Mild Dealumination

All previous research to remove aluminium from zeolite structures was done on powdered or granular zeolite, so the location of aluminium in the crystalline framework is well known. In this research work, and for the first time, we studied the mild dealumination process of binder-free zeolite Y. This kind of zeolite, BF-Y, contains new bonds formed between aluminium and other elements, which are formed especially between clay particles and zeolite crystals (seed) after crystallization of Y zeolite with a binder in sodium silicate solution. It is necessary to convert BF-Y zeolite from sodium to ammonium form before starting dealumination with acetic acid. During the ion exchange process, some of the aluminium is already removed from the zeolites framework (Sato et al., 2003). According to the results listed in Table 5, 92.5% of the sodium form BF was converted to ammonium form Y zeolite (BF-NH₄Y) after being subjected to ion exchange with NH₄NO₃ solution at 80°C for 4 hours. The prepared BF-NH₄Y is then dealuminated with commercial vinegar (0.75 M ethanoic acid) at 90°C for different periods of time. Table 6 shows the adsorption

characteristic, Si/Al ratio, and crystallinity percentage of modified binder-free Y zeolite (MBF-Y). Partially, a loss in crystallinity percentage of BF-Y was observed after dealumination, Figure 1d. It is obvious that the extraction of aluminium from the BF-Y framework causes a defect in the lattice (Qin et al., 2020). According to the XRD patterns, there were a few signs of amorphous structures or phase species forming in all frameworks after dealumination (Figure 1).

Table 5. Effect of the number of exchanges on the (% wt.) Na cation.

Time (h)	% Na ⁺ removed
1	52
2	76
3	85
4	92.5



4.4. Thermo Gravimetric Analysis (TGA):

The thermal stability and hydrophobicity of BF-Y and MBF-Y were investigated by TGA, (Figure 2). As can be seen from the

Figure 1. XRD patterns: (a) powdered NaY, (b) BF-Y synthesized after 40 hours' crystallization, (c) BF-Y synthesized after 45h crystallisation, and (d) BF-Y after 1.5 hours dealumination.

TGA curves, there are two main reasons for the weight loss of the samples. The first weight loss is due to releasing the physically adsorbed water on the surface of the zeolite samples. The BF-Y showed 20.37% of weight loss at (34 -200°C), and the MBF-Y showed 13.46% at (34 -200°C) . Results of the first weight loss suggest that the hydrophobicity of MBF-Y increased (Ayad, Hussein, & Al-Tabbakh, 2020). This suggestion is in good agreement with our expectations. The BF-Y sample starts the decomposition at 640°C, and MBF-Y starts the decomposition at temperatures more than 800°C, which means that the thermal stability of zeolite dramatically increases by mild extraction of aluminium atoms from its framework (Blakeman et al., 2014).

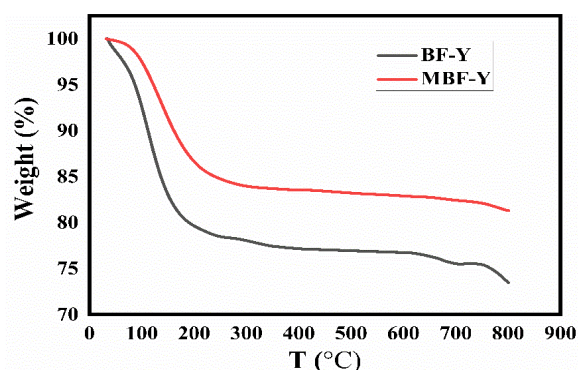


Figure 2. TGA curves of binder free zeolite before and after modification.

4.5. Scanning Electron Microscopy (SEM):

The surface morphology of the zeolite samples (FAU, granulated, and modified) was evaluated using SEM.

The microstructures of the untreated zeolite samples and the dealuminated (mild acid-treated) FAU are shown in Figure 3. The SEM images of the sample in Figure 3a clearly indicate the existence of the sample as a porous material, which is one of the important characteristics of powdered zeolite. The image produced at low magnification indicated the presence of clusters, most likely as a result of particle agglomeration on the surface of the sample. Different crystal shapes of Zeolite-Y FAU are most likely associated with different raw materials, modifications, and preparation methods used. The formation of additional pores was further confirmed by scanning electron microscope pictures of NaY with the binder, as shown in Figure 3b, which show that the surface of NaY with the binder contains many cracks bigger than those that appeared in the NaY powder form of zeolite. This is because of the formation of new secondary pore structures between kaolin clay particles and zeolite FAU crystals. It is clear from Figure 3c that there is a slight difference in surface shape, and this is due to the effect of the crystallization on the granules (mixture of clay and zeolite) and the conversion of clay into zeolite that occurred. The SEM images depicted the uniform distribution of all zeolitic samples, and the dealumination protocol did not produce a noticeable change in the zeolite crystalline structures (Figure 3d). This means no significant alterations in their particle sizes and crystal morphology occurred.

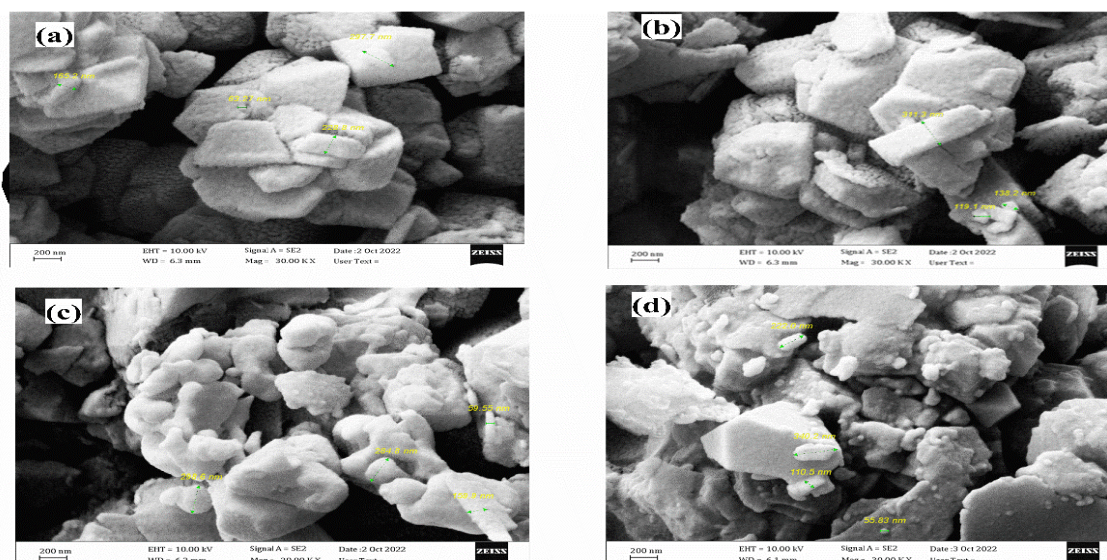


Figure 3. SEM micro graphs (a) powdered NaY, (b) GWB, (c) (BF-Y), and (d) MBF-Y obtained after 1.5h acid treatment.

Table 6. Influence of the mild dealumination time on the characterization of BF-Y zeolite

Sample	Dealumination time (h)	Adsorption capacity (mL.g ⁻¹)				Total pore volume (mL.g ⁻¹)	Crystallinity degree (%)
		Si/Al	A(benzene)	A(n-heptane)	A(water)		
GWB	0	4.433	0.122	0.131	0.240	0.362	38.12
BF-NH ₄ Y	0	4.015	0.310	0.320	0.190	0.430	98
BF-NH ₄ Y	0.5	5.309	0.232	0.262	0.212	0.444	97.67
	1	9.970	0.245	0.261	0.301	0.753	97.24
	1.5	8.397	0.317	0.280	0.316	0.630	96.00
	2	10.987	0.260	0.265	0.236	0.495	81.25
	2.5	11.352	0.243	0.263	0.216	0.459	79.00
	3	0.964	0.260	0.272	0.248	0.508	81.25

Table 7. Physicochemical characteristic of MBF-Y used as adsorbent for MB adsorption

Sample	Dealumination time(h)	Si/Al	BET surface area (M ² .g ⁻¹)	Total pore volume (mL.g ⁻¹)	Degree of crystallinity (%)
BF-NH ₄ Y	1.5	8.397	438.54	0.630	96.00

4.6. Adsorption Study

The binder free granules obtained after 1.5h acid treatment was employed as adsorbent for adsorption of MB. Table (7) shows the characteristic MBF-Y used as adsorbent.

4.6.1. Effect of Adsorbate Initial Concentration:

One of the most important factors in equilibrium investigations and for obtaining optimized studies to improve the pertinent values between pollutants in aqueous solution and adsorbents are initial concentration variations. Taking into account that the

concentration of dyes changes somewhat in actual environmental media, the effects of various MB concentrations were investigated. As can be seen in Figure 4a, the adsorption capacity of the MBF-Y was strongly impacted by the original dye concentration. MB

concentrations ranged from 6.5×10^{-6} to 2×10^{-5} M, while temperature, pH, and contact times remained constant across all determinations. The graph showed that the adsorption capacity increased along with a rise in the MB's initial concentration. As anticipated, the maximal adsorption capacity was reached at the highest dye concentration of 2×10^{-5} M. The reason for this is the fact that at higher MB concentrations, a greater number of MBF-Y active sites are surrounded by dye molecules. Figure 4b shows the effect of MB initial concentration on the percentage of dye removal. The results reveal that the percentage of dye removal increases as the initial concentration increases from 6.5×10^{-6} M to 8×10^{-6} M, then decreases at higher concentrations (8×10^{-6} M) to (2×10^{-5} M). The primary factor contributing to a decline in the percentage of MB removal at high dye concentrations may be competition between dye molecules for the scarce active site (Ali et al. 2021).

4.6.2. Effect of pH:

Surface charge, which is largely influenced by the fluid pH, is the most crucial factor in the adsorption of anionic and cationic dye

4.6.3. Effect of Adsorbent Dosage:

Adsorbent dosage is a crucial practical aspect of the adsorption technique that significantly affects the removal rate and reveals the cost-effectiveness of the batch process. Several tests were performed using various adsorbent amounts ranging from 0.01 to 0.02 g in 50 mL of 1×10^{-5} M MB solutions to determine the optimum MBF-Y amount required for adsorption at pH 7.8. Figure 6 shows the effect of MBF-Y dosage on the adsorption capacity of MB at equilibrium and the percentage of dye removal. All experiments were done at 25 °C for 80 min. It was found that the adsorption capacity decreased as the mass of MBF-Y zeolite increased. At an MBF-Y mass of 0.01 g, the maximum adsorption capacity of MB was found to be 4.33×10^{-5} mol. g⁻¹. This may be due to the fact that most of the binding sites of the MBF-Y appear to remain unsaturated when the amount of adsorbent in the solution exceeds the optimum value, which suggests reduced adsorption capacity and financial loss. By contrast to the adsorption capacity, the dye removal percentage increases with increasing the adsorbent dosage, and the efficiency of MB removal reaches about 99% at 0.02 g of MBF-Y dosage.

molecules. Therefore, in this research, the effect of the solution pH on the adsorption of cationic dye (MB) onto MBF-Y zeolite was investigated by using MB solution with pH values ranging from 3 to 11 and keeping other parameters such as temperature, initial concentration of dye, MBF-Y dose, and contact time constant. The results in Figure 5 show that the adsorption capacity, removal percentage of MB increase as the pH value of the solution increases. The maximum removal of MB (98%) was obtained at pH of 10.4, this may be due to the fact that at high pH values ($\text{pH} > \text{pH}_{\text{ZPC}}$) de protonation of MBF-Y acid sites takes place and the surface of MBF-Y becomes negatively charged which leads to greater attraction forces between the cationic dyes MB and MBF-Y (Idrees, Jamil, & Omer, 2022).

4.6.4. Effect of Contact Time:

Characterizing the adsorption mechanism requires knowledge of both the adsorption method's equilibrium reaction time and the rate at which equilibrium is achieved. Not only must an adsorbent achieve equilibrium quickly, but it must also favour adsorption as strongly as possible at that equilibrium. Adsorption of MB dye was performed over a time range of 0-80 min, at 25°C, a pH of 7.8, and (1×10^{-5} M) MB dye solution. Figure (7) illustrates the effect of contact time on the MB removal. The results show that the adsorption capacity of MBF-Y sharply increases after the first 5 minutes of the process, with about 77% of MB removed during this short time, and then gradually increases from 10-60 minutes. At around 60 minutes, the adsorption equilibrium was achieved.

4.6.5. Effect of Temperature

Temperature is one of the most important factors influencing the adsorption process. Therefore, the effect of temperature on the adsorption of MB on MBF-Y was studied at temperature of 25, 30,40 and 50°C, pH of 7.8, contact time 80min, and using MB solution of 1×10^{-5} M as initial concentration. Results are shown in Figure 8. As can be seen from Figure 8, the adsorption capacity of MB on MBF-Y decreases as temperature increases, which indicates that this adsorption process is of the physical type (physisorption) with a negative value of enthalpy change (ΔH). Furthermore, the decrease in adsorption capacity caused by increasing temperature could be attributed to a decrease in adsorptive forces between MB and MBF-Y, as it is known that the interaction forces, Vander Waal's decrease as temperature increases.

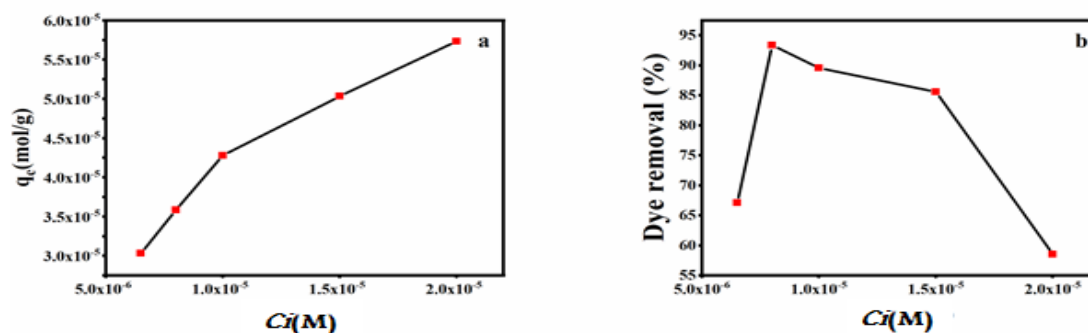


Figure 4. Effect of initial concentration (6.5×10^{-6} - 2×10^{-5}) M of MB on (a) adsorption capacity, (b) dye removal percentage

(conditions: T=25°C; contact time = 80min; pH=7.8; dosage=0.01g)

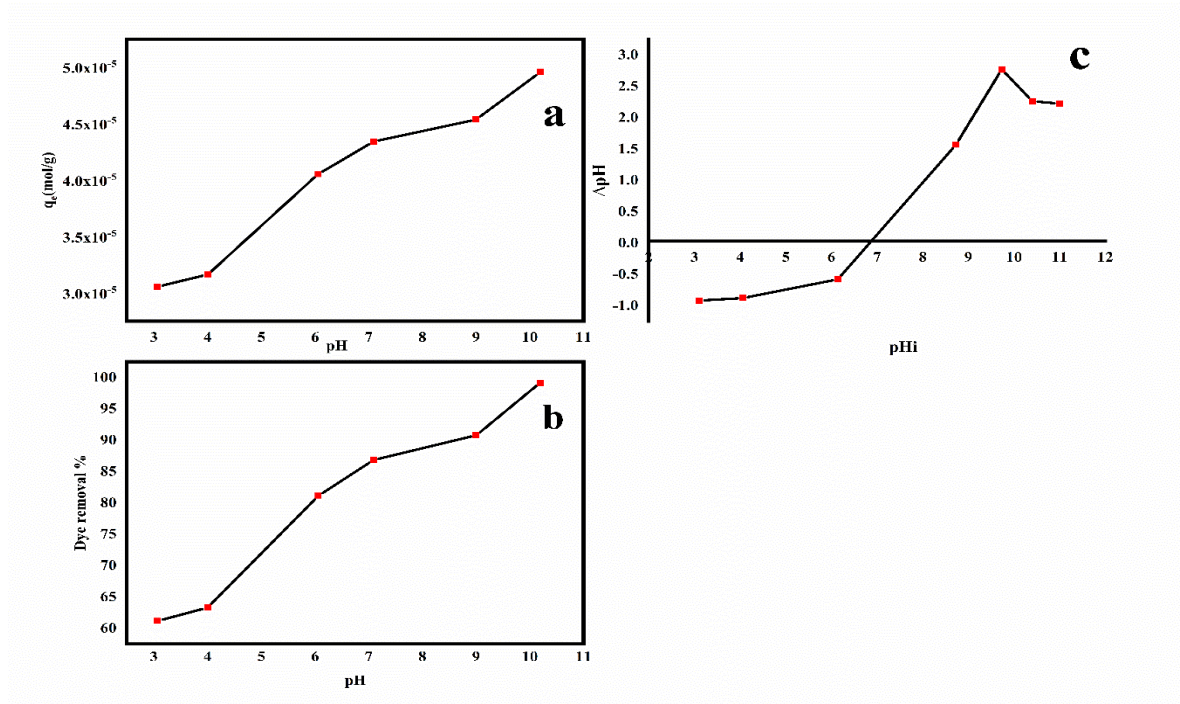


Figure 5 (a) impact of initial pH on adsorption capacity of MB on MBF-Y, (b) impact of initial pH on MB removal percentage, and, (c) the study of pHzc of the MBF-Y adsorbent. (conditions : T=25°C; initial concentration = 1×10^{-5} M; adsorbent dosage= 0.01g; contact time = 80min)

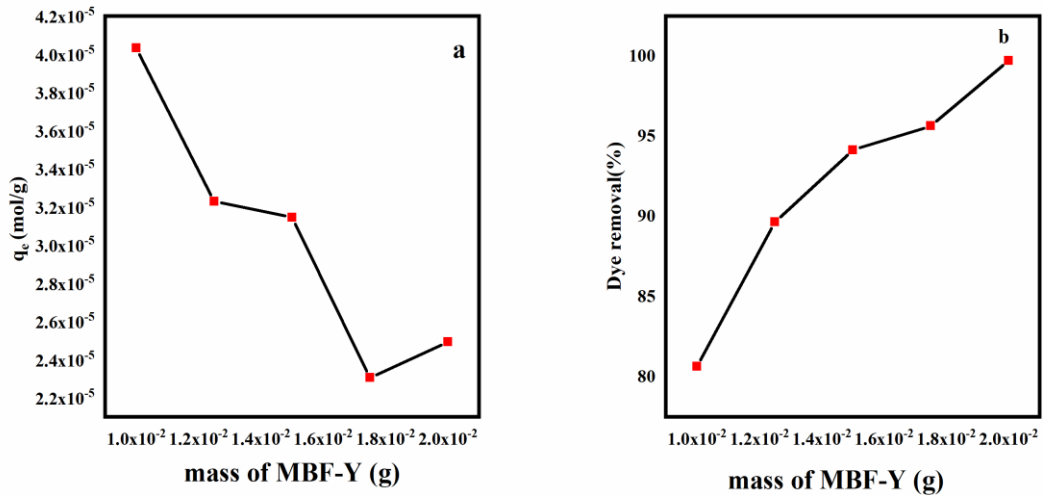


Figure 6. Effect of adsorbent dosage (0.01-0.02g) on MB adsorption onto MBF-Y on (a) adsorption capacity, (b) dye removal percentage (conditions : T=25°C; contact time = 80min; initial concentration= 1×10^{-5} M; pH=7.8)

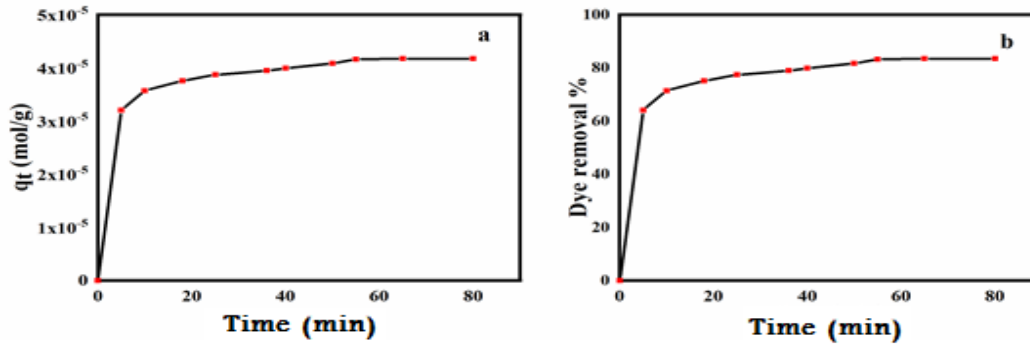


Figure 7 Effect of contact time (0-80min) on MB adsorption onto MBF-Y on (a) adsorption capacity, (b) dye removal percentage

(conditions : $T=25^{\circ}\text{C}$; initial concentration = $1 \times 10^{-5}\text{M}$; adsorbent dosage= 0.01g; $\text{pH}=7.8$)

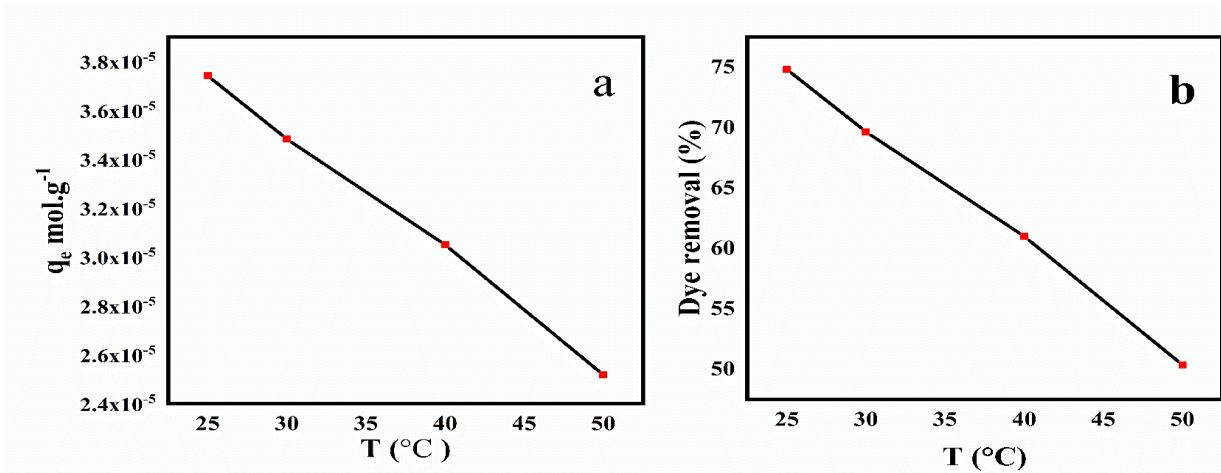


Figure 8. Effect of temperature(25-50°C) on MB adsorption onto MBF-Y on (a) adsorption capacity, (b) dye removal percentage

(conditions : contact time = 80min; initial concentration= $1 \times 10^{-5}\text{M}$; adsorbent dosage= 0.01g ; $\text{pH}=7.8$)

4.7. Adsorption Kinetics

In order to study the adsorption kinetics and mechanism of MB on MBF-Y, pseudo-first-order and pseudo-second-order models were employed. Equation (3) was used to represent the pseudo-first-order model, and equation (4) was used to represent the pseudo-second-order.

$$\ln (q_e - q_t) = \ln q_e - K_1 t \quad (3)$$

$$\frac{t}{q_t} = \frac{1}{k_2 q_e^2} + \frac{t}{q_e} \quad (4)$$

(Majid, AbdulRazak, & Noori, 2019),

Where q_e is the equilibrium adsorption in mol g⁻¹, q_t is the adsorption capacity after the time (t) in mol g⁻¹, k_1 is the first order specific rate constant (min⁻¹), and k_2 is the second-order specific rate constant, mol g⁻¹ min⁻¹. Linearized plots of pseudo-1st and 2nd order are shown in Figure (9). The fitted parameters are listed in Table 8. The value of R² for pseudo 1st order was 0.43854, and for pseudo 2nd-order, it was (0.99093). The value of

R² confirms that the adsorption of MB on MBF-Y zeolite follows pseudo second-order kinetics.

Table 8. Pseudo first order and pseudo second order parameters of MB adsorption onto MBF-Y.

Kinetic model	Parameters	Value
Pseudo first order	q_e (mol/g)	5.6503×10^{-3}
	K_1 (min ⁻¹)	0.1568
	R ²	0.43854
Pseudo second order	q_e (mol/g)	5.48081E-06
	K_2 (mol.g ⁻¹ .min ⁻¹)	1402664.26
	R ²	0.99093

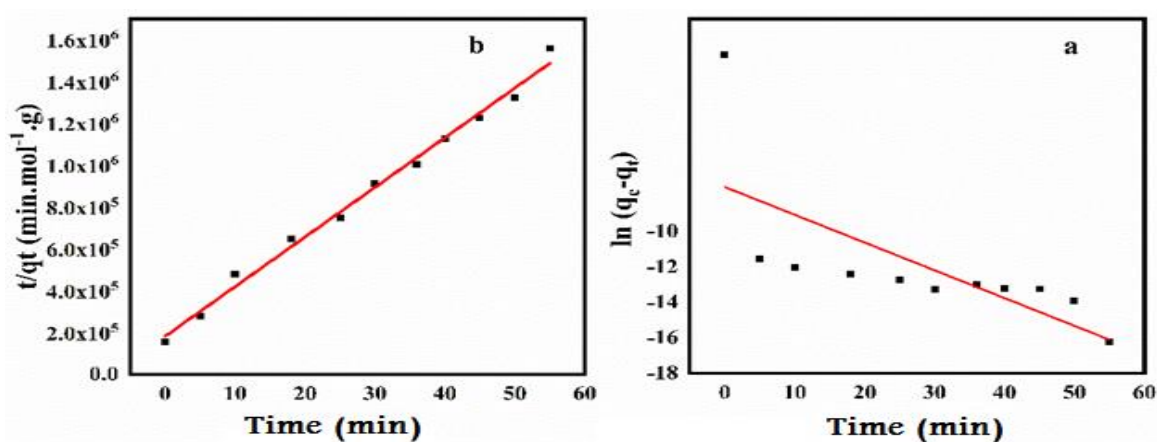


Figure 9. Adsorption kinetics models for MB adsorption onto MBF-Y, (a) pseudo first order, (b) pseudo second order (conditions: T=25C; initial concentration = 1×10^{-5} M; pH= 7.8; adsorbent dosage= 0.01g)

4.8.

4.9. Adsorption Thermodynamics

In order to better understand how temperature affects the adsorption process of MB onto MBF-Y, thermodynamic parameters such as a change in enthalpy (ΔH), entropy change (ΔS) and Gibbs free energy (ΔG), were calculated using equations (5), (6) and (7) (Lima et al., 2019).

$$\ln K_D = \frac{\Delta S}{R} - \frac{\Delta H}{RT} \quad (5)$$

$$K_D = \frac{q_e}{C_e} \quad (6)$$

$$\Delta G = -RT \ln K_D \quad (7)$$

where K_D is the adsorption equilibrium constant, R is the universal gas constant (J.mol⁻¹. K⁻¹), and T is the temperature in Kelvin. Figure (10) describes Van't Hoff plot of $\ln K_D$ versus $1/T$. The slope and intercept were used for calculating the values of ΔH and ΔS . From the data in Table (9), the value of enthalpy change, ΔH , is negative, which indicates that the adsorption of MB on the MBF-Y zeolite is exothermic; The negative value of (ΔS) indicates the decrease in the degree of randomness and the reduced possibility of accidental contacts between an adsorbent and a solution, and the negative value of (ΔG) indicates the adsorption process is spontaneous.

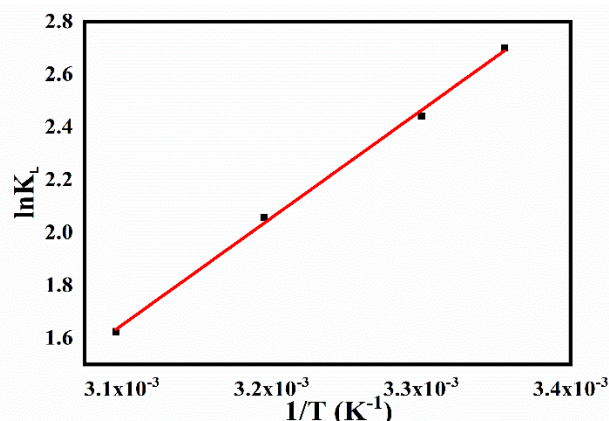


Figure 10 Van't Hoff plot (thermos dynamic diagram of MB adsorption onto MBF-Y)

Table 9. Thermodynamic parameters of MB adsorption onto MBF-Y

Temperature (K)	K _D	ΔG (KJ.mol ⁻¹)	ΔH (KJ.mol ⁻¹)	ΔS (KJ.mol ⁻¹ .K ⁻¹)	R ²
298	4.171369472	-6.68704	-33.817229	-0.09112402	0.99735
303	3.483094522	-6.14844			
313	3.049575074	-5.35131			
323	2.518459363	-4.36168			

4.10. Adsorption Isotherms

Capacities of adsorbents are usually determined by using equilibrium adsorption isotherms. In this study Langmuir, Freundlich, and Tempkin isotherm models were applied. The models are expressed by equations (8-10) respectively (Shikuku & Mishra, 2021).

$$\frac{C_e}{q_e} = \frac{C_e}{q_m} + \frac{1}{K_L q_m} \quad (8)$$

$$\ln q_e = \ln K_F + \frac{1}{n} \ln C_e \quad (9)$$

$$q_e = \frac{RT}{b_T} \ln K_T + \frac{RT}{b_T} \ln C_e \quad (10)$$

Where q_e is the amount of MB adsorbed at equilibrium (mol g⁻¹), C_e is the concentration of MB remained at equilibrium (M), q_m is the maximum amount of MB molecules adsorbed per unit mass of MBF-Y (mol g⁻¹), K_L is the Langmuir adsorption constant, K_F is Freundlich maximum adsorption capacity constant, n is the Freundlich adsorption intensity constant, b_T is the slope (J.mol⁻¹), K_T is the equilibrium binding constant of Tempkin. Figure (11) shows the fitted plots of these three isotherm models. The results are listed in Table (10)

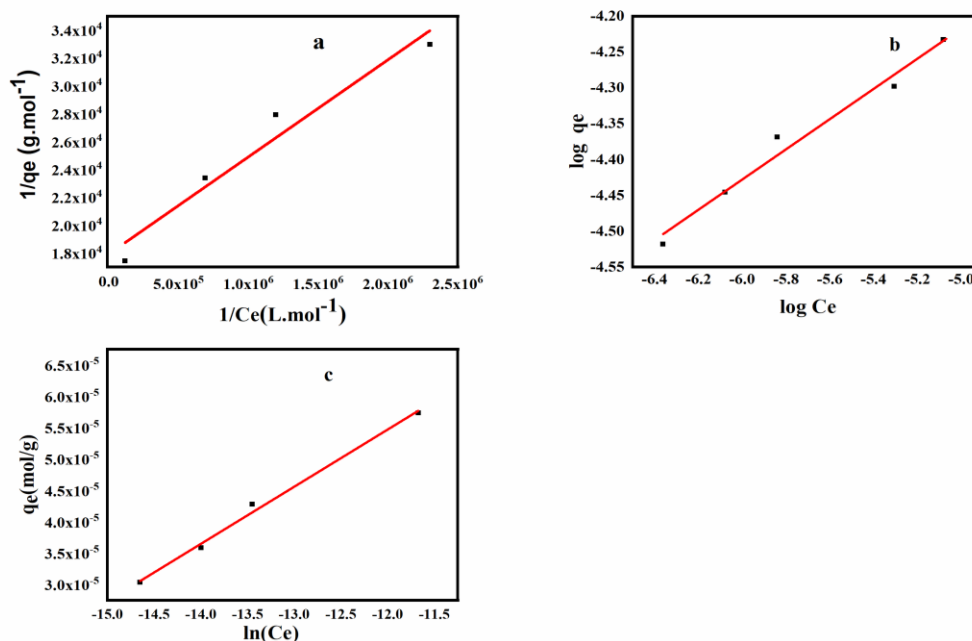


Figure 11. Adsorption isotherms of MB onto MBF-Y zeolite (a) Langmuir, (b) Freundlich, and (c) Tempkin isotherms

Table 11. Comparison of maximum adsorption capacities of MB onto various adsorbents.

No	Sample	qmax(mg.g ⁻¹)	Reference
1	Magnetic NaY Zeolite Composite	2.046	(Shirani et al. 2014)
2	Steam activated carbon from lantana camara stem	19.84	(Amuda et al. 2014)
3	Thermally Treated Natural Zeolites	0.13	(Senila et al. 2022)
4	Magnetic zeolites synthesized from recycled fly ash	16.533	(Supelano et al. 2020)
5	Zeolite/nickel ferrite/sodium alginate bio nanocomposite	54.054	(Bayat, Javanbakht, and Esmaili 2018)
6	Acid treated binder free granular Y zeolite	17.84	This work

5. CONCLUSION

We have demonstrated that to obtain adsorbents, BF-Y can be synthesized by crystallization of GWB in sodium silicate solution for 40 hours at 100°C and using a reaction mixture of 2.2 Na₂O. Al₂O₃. 6.5SiO₂. 155H₂O. BF-Y zeolite with high thermal and hydrothermal stability and increasing the Si/Al ratio is achieved by acid treatment (mild dealumination) of BF-NH₄Y samples at temperatures of 100 °C in dependence on time. XRD and adsorption capacity showed that the zeolite powder and BF-Y obtained are highly crystalline, and the molar SiO₂: Al₂O₃ ratio of the BF-Y sample was 4.01. The modified zeolite MBF-Y after 1.5 hours showed a Si/Al ratio higher than 5, high N₂ adsorption, and BET surface area and total pore volume determined to be 438.54 m² g⁻¹ and 0.630 mL g⁻¹, respectively. MBF-Y was investigated as an adsorbent for water-soluble MB dye. The

effect of a number of factors, such as the initial concentration of MB, the MBF-Y dosage, contact time, and temperature, on the adsorption process, was investigated, and it was found that the adsorption of MB onto MBF-Y was dependent on the initial concentration of MB, the MBF-Y dosage, contact time, and temperature. Pseudo-1st order and pseudo-2nd order was applied to study the adsorption kinetics, and the adsorption process was found to follow pseudo-2nd order with (R²=0.99). Three well-known adsorption isotherms, Langmuir, Freundlich, and Tempkin, were applied to discuss the adsorption behavior, and all three isotherms showed favorable results for the process, with correlation factors of 0.93416, 0.97133, and 0.99171, respectively.

ACKNOWLEDGEMENTS

The authors thankfully acknowledge Mr. Shinwar A. Idrees for his helpful collaboration.

REFERENCES

- Ali, L I Abd, Hani K Ismail, Hasan F Alesary, and H Y Aboul-Encin. 2021. "A Nanocomposite Based on Polyaniline, Nickel and Manganese Oxides for Dye Removal from Aqueous Solutions." *International Journal of Environmental Science and Technology* 18: 2031–50.
- Amuda, Omotayo Sarafadeen et al. 2014. "Adsorption of Methylene Blue from Aqueous Solution Using Steam-Activated Carbon Produced from Lantana Camara Stem." *Journal of Environmental Protection* 5(13): 1352.
- Ayad, Zahraa, Hussein Q. Hussein, and Ban A. Al-Tabbakh. 2020. "Synthesis and Characterization of High Silica HY Zeolite by Basicity Reduction." *AIP Conference Proceedings* 2213(March).
- Bayat, Mahsa, Vahid Javanbakht, and Javad Esmaili. 2018. "Synthesis of Zeolite/Nickel Ferrite/Sodium Alginate Bionanocomposite via a Co-Precipitation Technique for Efficient Removal of Water-Soluble Methylene Blue Dye." *International Journal of Biological Macromolecules* 116(2017): 607–19. <https://doi.org/10.1016/j.ijbiomac.2018.05.012>.
- Beyer, Hermann K. 2002. "Dealumination Techniques for Zeolites." In *Post-Synthesis Modification I*, Springer, 203–55.
- Blakeman, Philip G et al. 2014. "The Role of Pore Size on the Thermal Stability of Zeolite Supported Cu SCR Catalysts." *Catalysis Today* 231: 56–63.
- Grigorieva, N G et al. 2019. "A Hierarchically Zeolite Y for the N-Heterocyclic Compounds Synthesis." *Journal of Saudi Chemical Society* 23(4): 452–60.
- Idrees, Shinwar A, Lazgin A Jamil, and Khalid M Omer. 2022. "Silver-Loaded Carbon and Phosphorous Co-Doped Boron Nitride Quantum Dots (Ag@CP-BNQDs) for Efficient Organic Waste Removal: Theoretical and Experimental Investigations." *ACS omega* 7(42): 37620–28.
- Ihaddaden, Soraya, Dihia Aberkane, Abdelhamid Boukerroui, and Didier Robert. 2022. "Removal of Methylene Blue (Basic Dye) by Coagulation-Flocculation with Biomaterials (Bentonite and Opuntia Ficus Indica)." *Journal of Water Process Engineering* 49: 102952. <https://www.sciencedirect.com/science/article/pii/S2214714422003968>.
- Ismail, Hani K et al. 2022. "Synthesis of a Poly (p-Aminophenol)/Starch/Graphene Oxide Ternary Nanocomposite for Removal of Methylene Blue Dye from Aqueous Solution." *Journal of Polymer Research* 29(5): 159.
- Li, Qiang et al. 2010. "Influence of Synthesis Parameters on the Crystallinity and Si/Al Ratio of NaY Zeolite Synthesized from Kaolin." *Petroleum Science* 7: 403–9.
- Lima, Eder C, Ahmad Hosseini-Bandegharai, Juan Carlos Moreno-Piraján, and Ioannis Anastopoulos. 2019. "A Critical Review of the Estimation of the Thermodynamic Parameters on Adsorption Equilibria. Wrong Use of Equilibrium Constant in the Van't Hoof

- Equation for Calculation of Thermodynamic Parameters of Adsorption.” *Journal of molecular liquids* 273: 425–34.
- Liu, Lin et al. 2015. “Adsorption Removal of Dyes from Single and Binary Solutions Using a Cellulose-Based Bioadsorbent.” *ACS Sustainable Chemistry and Engineering* 3(3): 432–42.
- Liu, Xinmei, Zifeng Yan, Huaiping Wang, and Yantuo Luo. 2003. “In Situ Synthesis of NaY Zeolite with Coal-Based Kaolin.” *Journal of Natural Gas Chemistry* 12(1): 63–70.
- Majid, Zaiyanb, Adnan A. AbdulRazak, and Wallaa Abdul Hadi Noori. 2019. “Modification of Zeolite by Magnetic Nanoparticles for Organic Dye Removal.” *Arabian Journal for Science and Engineering* 44(6): 5457–74. <https://doi.org/10.1007/s13369-019-03788-9>.
- McDaniel, C V, and P K Maher. 1968. “Molecular Sieves.” *Society of Chemical Industry, London* 186.
- Najar, Hanene, Mongia Saïd Zina, and Abdelhamid Ghorbel. 2010. “Study of the Effect of the Acid Dealumination on the Physico-Chemical Properties of Y Zeolite.” *Reaction Kinetics, Mechanisms and Catalysis* 100(2): 385–98.
- Omar, Hanan, Adel El-Gendy, and Khairia Al-Ahmary. 2018. “Bioremoval of Toxic Dye by Using Different Marine Macroalgae.” *Turkish Journal of Botany* 42(1): 15–27.
- Pavlov, M. L. et al. 2015. “Synthesis of Ultrafine and Binder-Free Granular Zeolite y from Kaolin.” *Petroleum Chemistry* 55(7): 552–56.
- Peng, Mei Xun, Zheng Hong Wang, Shao Hua Shen, and Qiu Guo Xiao. 2015. “Synthesis, Characterization and Mechanisms of One-Part Geopolymeric Cement by Calcining Low-Quality Kaolin with Alkali.” *Materials and Structures* 48: 699–708.
- Peng, Na et al. 2016. “Superabsorbent Cellulose-Clay Nanocomposite Hydrogels for Highly Efficient Removal of Dye in Water.” *ACS Sustainable Chemistry and Engineering* 4(12): 7217–24.
- Ptáček, Petr, Františka Frajkorová, František Šoukal, and Tomáš Opravil. 2014. “Kinetics and Mechanism of Three Stages of Thermal Transformation of Kaolinite to Metakaolinite.” *Powder Technology* 264: 439–45. <http://dx.doi.org/10.1016/j.powtec.2014.05.047>.
- Qin, Zhengxing et al. 2020. “Defect-Assisted Mesopore Formation during Y Zeolite Dealumination: The Types of Defect Matter.” *Microporous and Mesoporous Materials* 303: 110248.
- Rashidi, H. Reza et al. 2015. “Synthetic Reactive Dye Wastewater Treatment by Using Nano-Membrane Filtration.” *Desalination and Water Treatment* 55(1): 86–95.
- Rida, Kamel, Sarra Bouraoui, and Selma Hadnine. 2013. “Adsorption of Methylene Blue from Aqueous Solution by Kaolin and Zeolite.” *Applied Clay Science* 83–84: 99–105. <http://dx.doi.org/10.1016/j.clay.2013.08.015>.
- Sato, Koichi et al. 2003. “Structural Changes of Y Zeolites during Ion Exchange Treatment: Effects of Si/Al Ratio of the Starting NaY.” *Microporous and mesoporous materials* 59(2–3): 133–46.
- Senila, Lacrimioara et al. 2022. “Removal of Methylene Blue on Thermally Treated Natural Zeolites.” *Analytical Letters* 55(2): 226–36. <https://doi.org/10.1080/00032719.2021.1922431>.
- Shikuku, Victor O., and Trilochan Mishra. 2021. “Adsorption Isotherm Modeling for Methylene Blue Removal onto Magnetic Kaolinite Clay: A Comparison of Two-Parameter Isotherms.” *Applied Water Science* 11(6): 1–9. <https://doi.org/10.1007/s13201-021-01440-2>.
- Shirani, Mahboube, Abolfazl Semnani, Hedayat Haddadi, and Saeed Habibollahi. 2014. “Optimization of Simultaneous Removal of Methylene Blue, Crystal Violet, and Fuchsine from Aqueous Solutions by Magnetic NaY Zeolite Composite.” *Water, Air, and Soil Pollution* 225(8).
- Shirazi, L., E. Jamshidi, and M. R. Ghasemi. 2008. “The Effect of Si/Al Ratio of ZSM-5 Zeolite on Its Morphology, Acidity and Crystal Size.” *Crystal Research and Technology* 43(12): 1300–1306.
- Simancas, Raquel et al. 2021. “Recent Progress in the Improvement of Hydrothermal Stability of Zeolites.” *Chemical Science* 12(22): 7677–95.
- Supelano, G. I. et al. 2020. “Synthesis of Magnetic Zeolites from Recycled Fly Ash for Adsorption of Methylene Blue.” *Fuel* 263(November 2019): 116800. <https://doi.org/10.1016/j.fuel.2019.116800>.
- Tsai, Wen Tien, Kuo Jong Hsien, and Hsin Chieh Hsu. 2009. “Adsorption of Organic Compounds from Aqueous Solution onto the Synthesized Zeolite.” *Journal of Hazardous Materials* 166(2–3): 635–41.
- Wang, Shaobin, and Huiting Li. 2007. “Kinetic Modelling and Mechanism of Dye Adsorption on Unburned Carbon.” *Dyes and Pigments* 72(3): 308–14.
- Wu, Huifang, and Shihe Wang. 2012. “Impacts of Operating Parameters on Oxidation-Reduction Potential and Pretreatment Efficacy in the Pretreatment of Printing and Dyeing Wastewater by Fenton Process.” *Journal of Hazardous Materials* 243: 86–94. <http://dx.doi.org/10.1016/j.jhazmat.2012.10.030>.